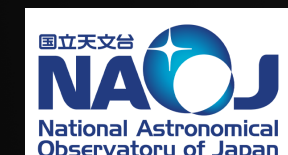
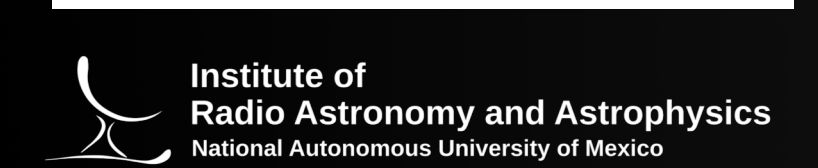


5 au Imaging of the Dust Polarization in HL Tau: Gaps and Rings Revealed



Leslie Looney^a, Ian Stephens^b, Manuel Fernández-Lopez^c, Zhe-Yu Daniel Lin^d, Zhi-Yun Li^d, Haifeng Yang^e, Carlos Carrasco-González^f, Rachel Harrison^{a,g}, Akimasa Katoka^h, Satoshi Okuzumiⁱ, & Ryo Tazaki^j

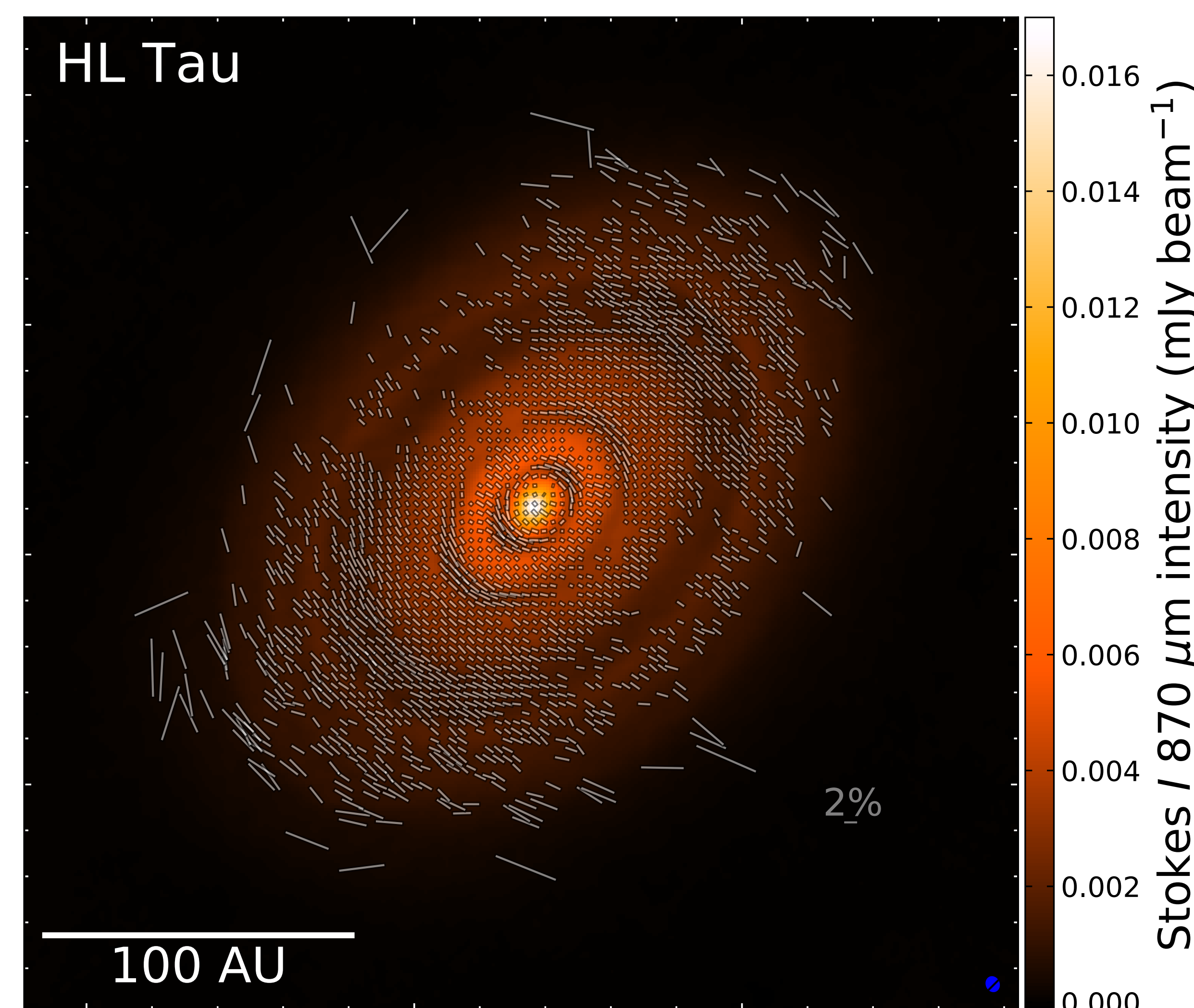


Fig 1: 870 micron continuum emission (RMS noise level of 17.3 $\mu\text{Jy}/\text{bm}$) in color scale with overlaid polarization morphology line segments (polarization RMS noise level of 8.5 $\mu\text{Jy}/\text{bm}$). The length of the segments are proportional to the percent of polarized light, with a 2% scale bar shown toward the bottom right. An illustrative beam is shown as a blue ellipse in the bottom right (0.49 au size).

1. Polarization of HL Tau at 870 microns

- HL Tau is a transitional Class I/Class II YSO⁽¹⁾ at 147 pc⁽²⁾ with a likely age <1Myr⁽³⁾.
- First high resolution polarization image (Fig 1) with ~1000 independently sampled polarization measurements resolving the rings and the gaps; the most spatially sampled circumstellar disk in polarization to date.
- Polarization generally aligned along the minor axis (as expected for dust scattering)⁽⁴⁾, but there is a clear and significant azimuthal component, particularly in the gaps.
- Polarized fractions and intensities are larger along the major axis than the minor axis.
- The most highly polarized emission is in the gaps, not the rings— ~3% in the gaps and often <1% in the rings.
- A new 8th ring is detected the continuum emission (Fig 2) at 107.5 au.

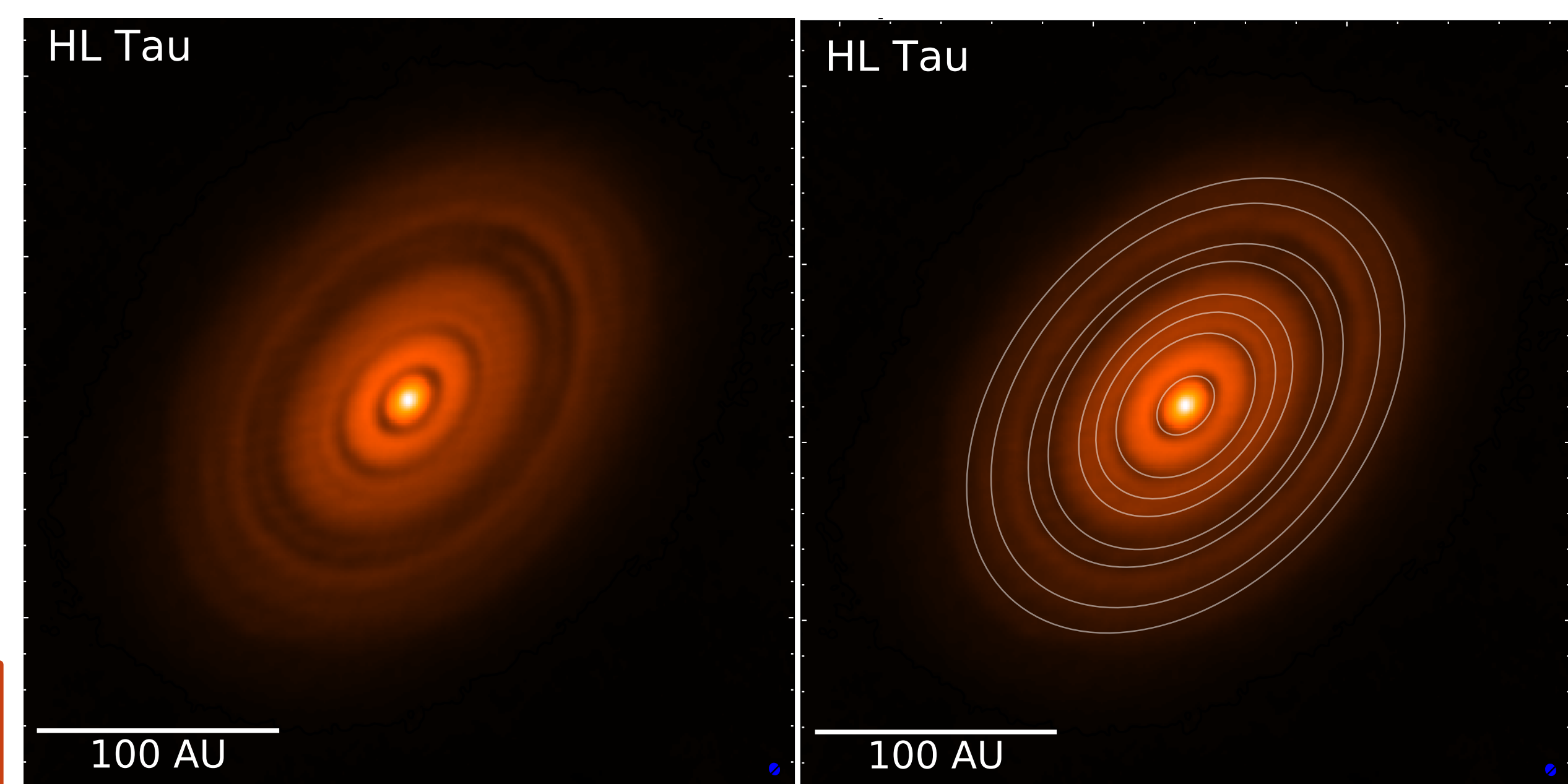


Fig 2: 870 micron continuum image of HL Tau. The right has overlaid ellipses to indicate the gaps. An 8th gap is detected for the first time.

2. Multiwavelength Polarization of HL Tau

- HL Tau polarization morphology (Fig 3) is strongly dependent on observing wavelength⁽⁴⁾.
- 870 micron polarization, parallel to disk minor axis, is dominated by dust self-scattering with dust grains $a_{\text{max}} \sim 100$ microns⁽⁴⁾.
- 3mm polarization, an azimuthal pattern, is dominated by aligned dust grains⁽⁵⁾; the azimuthal alignment mechanism is still unknown but either mechanical or aerodynamical alignment^(5,6). The transition with wavelength is due to optical depth⁽⁵⁾.

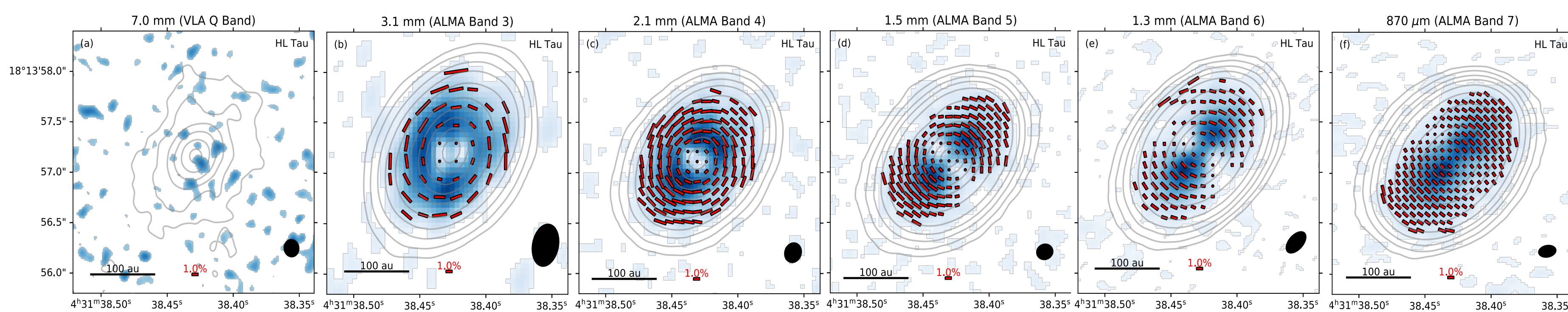


Fig 3: Multiwavelength observations of HL Tau polarization at lower resolution than Fig 1. In all cases, the contours are the total continuum emission, the color scale is the polarized emission, and the line segments are the polarization direction with the length representing 1% percent polarization marked with the scale bar given in each panel. An illustrative beam is shown as an ellipse in the bottom right.

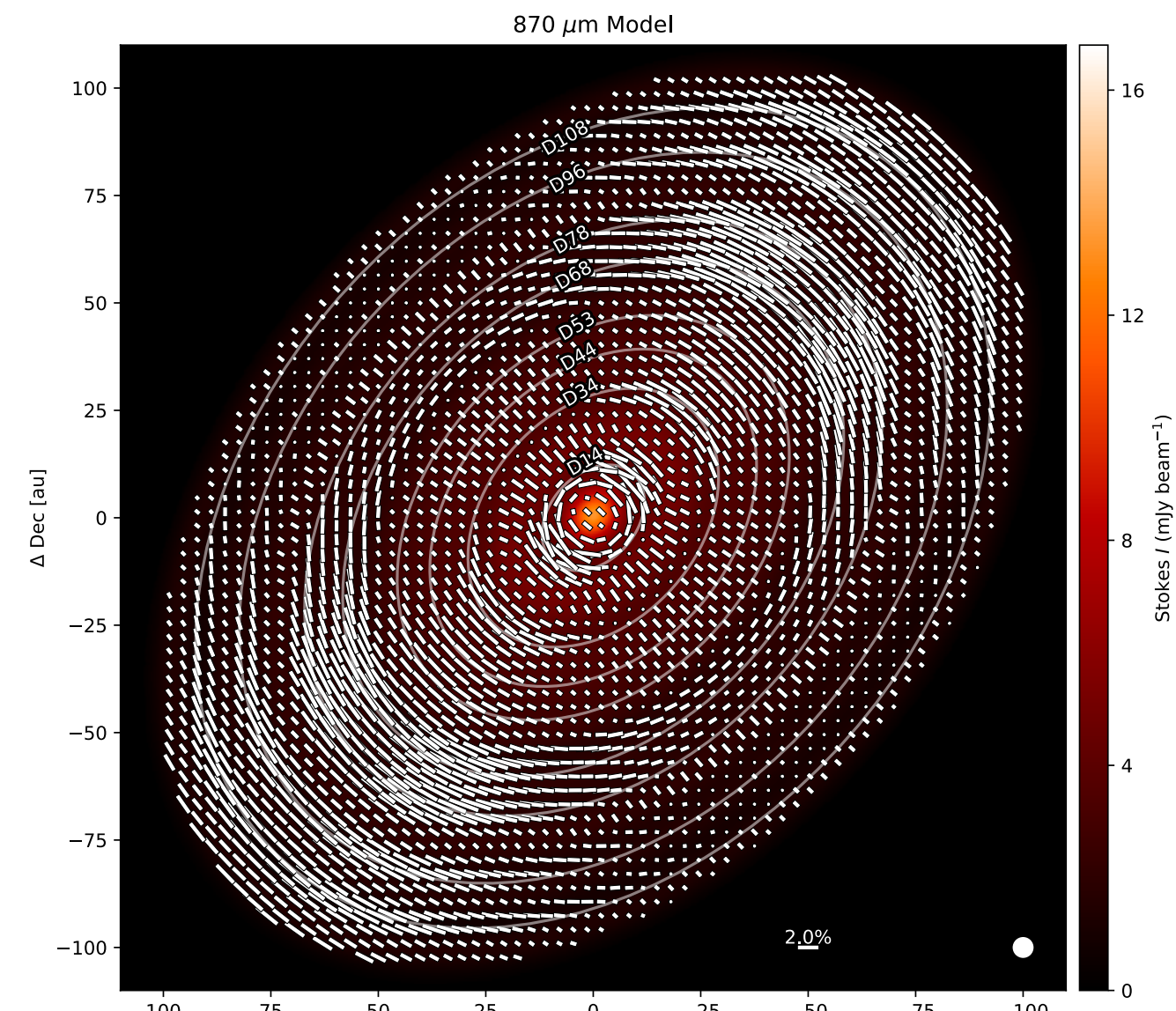


Fig 4: Model of the polarization in HL Tau using a combination of dust self-scattering from dust grains with an $a_{\text{max}} \sim 100$ microns and dust grains aligned in the disk azimuthally.

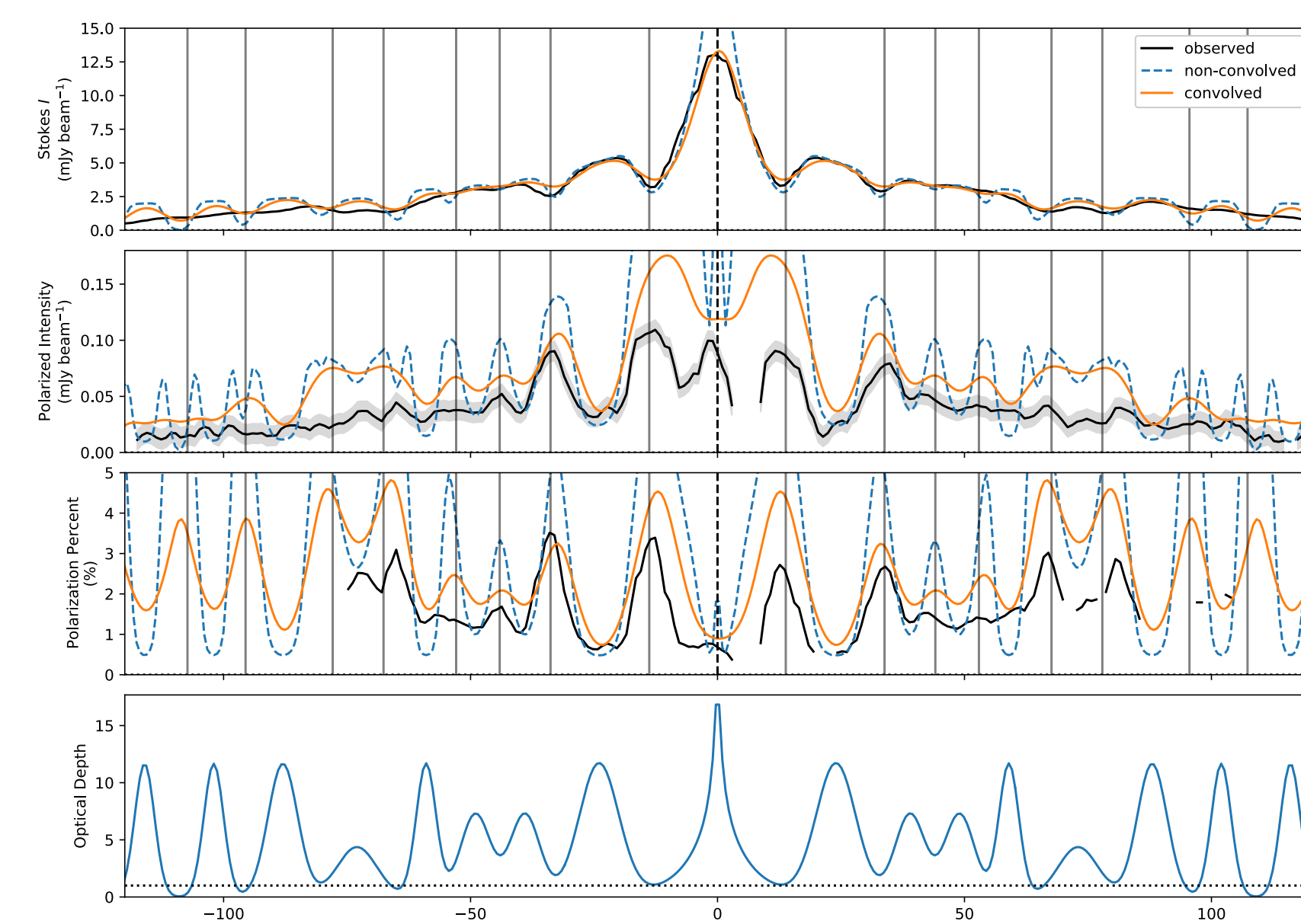


Fig 5: Comparisons of the profiles along the major axis between the observation and model (with and without beam convolution).

3. Polarization modeling of HL Tau

- Models with scattered light only could not fit the Fig 1 polarization observations, both dust self-scattering and aligned grains must be included (Fig 4 & 5).
- Prolate dust grains with a maximum effective size of $a_{\text{max}} \sim 100$ microns provide best fit.
- Grain alignment is such that the long axis of a rotating grain is aligned azimuthal around the disk, which is expected for either mechanical or aerodynamical alignment.
- To match the polarization fraction levels, an intrinsic polarization between 10% and 15% is needed, as beam averaging reduces gap polarization levels (Fig 5).
- Tension still remains between the dust grain a_{max} necessary to match the self-scattering polarization and that needed for the measured dust opacity with wavelength. Multi-wavelength observations at similar resolution are needed to unravel effects due to several different parameters, including grain size, composition, albedo, reflectivity, alignment, and intrinsic polarization.

References: 1. Weintraub+ 1995, ApJL, 452, L141; 2. Galli+ 2018, MNRAS, 877, L50; 3. Kristensen & Dunham 2018, A&A, 618,158; 4. Stephens+ 2017, ApJ, 851, 55; 5. Li+ 2022, MNRAS, 512, 3922; 6. Yang+ 2019, MNRAS, 483, 2371

a. University of Illinois, b. Worcester State University c. Instituto Argentino de Radioastronomía, d. University of Virginia, e. Peking University, f. National Autonomous University of Mexico, g. Monash University, h. National Astronomical Observatory of Japan, i. Tokyo Institute of Technology, j. Tohoku University